



Published in final edited form as:

*Neurorehabil Neural Repair*. 2008 ; 22(3): 262–278. doi:10.1177/1545968307308550.

## Nogo-66 Receptor Antagonist Peptide (NEP1-40) Administration Promotes Functional Recovery and Axonal Growth After Lateral Funiculus Injury in the Adult Rat

Y. Cao, MD, J. S. Shumsky, PhD, M. A. Sabol, R. A. Kushner, S. Strittmatter, PhD, F. P. T. Hamers, PhD, D. H. S. Lee, PhD, S. A. Rabacchi, PhD, and M. Murray, PhD

Department of Neurobiology and Anatomy, Drexel University College of Medicine, Philadelphia, PA (YC, JSS, MAS, RAK, MM); Department of Neurology, Yale University, New Haven, CT (SS); Department of Physical Medicine and Rehabilitation, Rudolf Magnus Institute of Neuroscience, University Medical Center, Utrecht, the Netherlands (FPTH); Department of Neuro-degeneration, Biogen-IDEC, Inc, Cambridge, MA; Lundbeck Research, Paramus, NJ (DHLS, SAR)

### Abstract

**Objective**—The myelin protein Nogo inhibits axon regeneration by binding to its receptor (NgR) on axons. Intrathecal delivery of an NgR antagonist (NEP1-40) promotes growth of injured corticospinal axons and recovery of motor function following a dorsal hemisection. The authors used a similar design to examine recovery and repair after a lesion that interrupts the rubrospinal tract (RST).

**Methods**—Rats received a lateral funiculotomy at C4 and NEP1-40 or vehicle was delivered to the cervical spinal cord for 4 weeks. Outcome measures included motor and sensory tests and immunohistochemistry.

**Results**—Gait analysis showed recovery in the NEP1-40-treated group compared to operated controls, and a test of forelimb usage also showed a beneficial effect. The density of labeled RST axons increased ipsilaterally in the NEP1-40 group in the lateral funiculus rostral to the lesion and contralaterally in both gray and white matter. Thus, rubrospinal axons exhibited diminished dieback and/or growth up to the lesion site. This was accompanied by greater density of 5 HT and calcitonin gene-related peptide axons adjacent to and into the lesion/matrix site in the NEP1-40 group.

**Conclusions**—NgR blockade after RST injury is associated with axonal growth and/or diminished dieback of severed RST axons up to but not into or beyond the lesion/matrix site, and growth of serotonergic and dorsal root axons adjacent to and into the lesion/matrix site. NgR blockade also supported partial recovery of function. The authors' results indicate that severed rubrospinal axons respond to NEP1-40 treatment but less robustly than corticospinal, raphe-spinal, or dorsal root axons.

### Keywords

Spinal cord injury; Rubrospinal tract; NEP1-40

---

Adult mammalian central nervous system (CNS) neurons do not spontaneously regenerate their axons. Contributors to this failure include the local environment of both the normal and injured adult CNS, which contains inhibitors that constitute a biochemical and physical barrier to regeneration.<sup>1</sup> Three molecules associated with myelin have been identified: NogoA,<sup>2–5</sup>

myelin-associated glycoprotein (MAG),<sup>6,7</sup> and oligodendrocyte-myelin glycoprotein (OMgp).<sup>8,9</sup> Nogo has 3 variants: NogoA, NogoB, and NogoC. NogoA is mainly expressed in the CNS, whereas the other 2 are more widely expressed outside the CNS. NogoA possesses a transmembrane loop region, Nogo66, which inhibits neurite outgrowth.<sup>10,11</sup> The Nogo-66 receptor, NgR1,<sup>12</sup> is a glycosylphosphatidylinositol-linked cell surface receptor that contains a leucine-rich repeat motif that also interacts with MAG<sup>13-15</sup> and OMgp.<sup>15,16</sup> All 3 myelin molecules bind to NgR1 in a complex with p75 neurotrophin receptor and a leucine-rich repeat transmembrane protein LINGO-1, which act to transduce the inhibitory signal across the cell membrane.<sup>16-18</sup> TAJ/TROY, an orphan tumor necrosis factor receptor family member, can also serve as an alternative coreceptor for NgR in place of p75.<sup>19,20</sup>

Strategies that neutralize or block the effects of NogoA have been successful in promoting repair and recovery of function after spinal cord injury (SCI). (1) A monoclonal antibody against NogoA (IN-1), when administered to spinal cord-injured rats, enabled regeneration and/or sprouting from corticospinal axons and partial recovery of function.<sup>21-23</sup> (2) An NgR competitive antagonist, NEP1-40 (Nogo66 residue 1-40), binds to the leucine-rich region of the receptor and also blocks the inhibitory effect of Nogo.<sup>11</sup> Intrathecal administration of NEP1-40 induced regenerative growth of corticospinal axons and partial recovery of function after dorsal hemisection injury in adult rats.<sup>11</sup> Delayed systemic delivery of NEP1-40 showed similar results in injured adult mice.<sup>24</sup> (3) Administration of NgR(310) ecto-F, an ecto-domain of the rat NgR (27-310) fused to a rat IgG, into rats with thoracic dorsal hemisections, resulted in improved open field locomotion and axonal sprouting of corticospinal fibers.<sup>25</sup> In a combined treatment with methylprednisolone, the recovery of locomotor function and axonal sprouting was more pronounced compared to either treatment alone.<sup>26</sup>

Another descending pathway, the rubrospinal tract (RST), is also implicated in motor function and the control of forelimb movements. Damage to the lateral funiculus destroys the RST but spares the corticospinal tract, and produces deficits in forelimb function that can be improved by therapeutic transplants.<sup>27,28</sup> This study was designed to evaluate the effectiveness of NEP1-40 delivered intrathecally to the spinal cord on the recovery of function and axonal growth following a lateral funiculotomy. We tested several motor and sensorimotor behaviors and used tracing methods to identify changes in patterns of descending and primary afferent projections.

## MATERIALS AND METHODS

### Subjects

Fifteen adult female Sprague-Dawley rats (250–300 g) were prepared as experimental animals. The animals were housed in pairs, in standard cages, with free access to food and water under a 12:12-hour light cycle and in conditions of controlled temperature and humidity. Seven unoperated animals were used as normal controls for gait analysis. All procedures involving animals in this study were approved by the Drexel University College of Medicine's Institutional Animal Care and Use Committee and conformed to NIH guidelines.

### Experimental Groups

Seven animals were prepared as operated control animals (op-controls) and 8 as an NEP1-40 treatment (NEP1-40) group. Both groups received first an intrathecal catheterization and 3 days later a right lateral funiculotomy at the C4 level. This 2-stage operative procedure was used because it was less stressful to the animals. An osmotic minipump was connected to the catheter immediately following the funiculotomy. The op-control group received an intrathecal delivery of vehicle that contained 97.5% PBS plus 2.5% DMSO, and the NEP1-40 group received an

intrathecal administration of 500  $\mu\text{M}$  NEP1-40 dissolved in 97.5% PBS plus 2.5% DMSO, delivered by minipump at 0.3  $\mu\text{l/h}$  for 28 days.

## Surgical Procedures

**Intrathecal Catheterization**—Catheters were implanted 3 days before the lateral funiculotomy. Rats were anesthetized with isoflurane and mounted in a stereotaxic instrument. A midline skin incision was extended from a line between the ears to about 1 cm caudal, and the atlanto-occipital membrane was exposed. The membrane was pierced using a bent 22-gauge needle, and a 2-mm lateral incision was made in the membrane. An intrathecal catheter (Marsil Scientific, San Diego, CA) was used to deliver drug or vehicle. The catheter consisted of 3 sections of polyethylene tubing, 0.5 cm PE60 tube joined to 4 cm PE10, which was joined to a 6.0 cm PE5. Four incisions made with #11 surgical blade 1.5 cm from the junction of the PE5 and PE10 tubing allowed delivery of drug or vehicle from the reservoir to the dorsal surface of the C4 spinal cord. The PE5 tubing was gently inserted into the subarachnoid space surrounding the spinal cord. The junction of PE5 and PE10 tubing was secured to the adjacent muscle. The tip of the PE60 tubing was sealed to prevent leakage of CSF, and the PE10-PE60 portion of the catheter was embedded subcutaneously. Osmotic pumps were loaded with vehicle or NEP1-40 solution at room temperature and submerged in 0.9% saline at 37°C for 40 hours to reach a constant delivery rate. Following the lateral funiculotomy, the catheter was connected to the osmotic minipump outlet (Alzet 2004, ~240  $\mu\text{l}$  volume, 0.30  $\mu\text{l/h}$ , 28-day delivery) and secured to the muscles with 4-0 silk suture. Because of the distance between the osmotic minipump and the lesion site, NEP1-40 or vehicle reached the lesion site about 12 hours after the insertion. We adapted the drug concentration and delivery method from that described by GrandPré et al.<sup>11</sup> The intrathecal catheterization was modified from the method described by Yaksh<sup>29</sup> by the addition of the PE5 tubing. This modification was made to diminish the mechanical damage often caused to the cervical spinal cord by the catheter.<sup>30</sup> The pump was removed at the end of the experiment, 56 days after the implantation, and evacuated using a 27-gauge filling tube, provided by Alzet to test for residual NEP1-40; no NEP1-40 remained in any of the pumps.

**Lateral Funiculotomy**—Three days following the catheter implantation, rats were anesthetized with an intraperitoneal injection of acepromazine maleate (0.7 mg/kg; Fermenta Animal Health Co, Kansas City, MO), ketamine (95 mg/kg, Fort Dodge Animal Health, Fort Dodge, IA), and xylazine (10 mg/kg; Bayer Co, Shawnee Mission, KS). A laminectomy at the C3–4 level exposed one segment of spinal cord. At this time, the intrathecal catheter outlet was positioned correctly above the spinal cord in all experimental animals with no detectable damage to the cord. A 30G needle was used to open the dura and pia mater, and a shallow incision was made in the right dorsal spinal cord. A fine-tipped microaspirator was used to extend the lesion laterally and ventrally. This lesion interrupted the lateral funiculus, including the right rubrospinal tract, and extended into the gray matter.<sup>27</sup> After hemostasis was achieved, 3  $\mu\text{l}$  of Vitrogen, a collagen matrix (Cohesion, Palo Alto, CA), was injected into the lesion site of each animal to fill the cavity. Vitrogen was used because it persists within the cavity and provides a permissive substrate for axonal growth.<sup>31,32</sup> The dura was closed with interrupted 9-0 silk sutures, and the muscles and skin were closed in layers. Animals that developed autophagy during the experimental period were treated daily, as necessary, with topical triple antibiotic ointment (CVS, Inc, Woonsocket, RI).

**Anterograde BDA Labeling**—Following 8 weeks of behavioral testing, animals were anesthetized and positioned in a stereotaxic apparatus, and the brain was exposed and 1  $\mu\text{l}$  of 10% BDA (Molecular Probes, Eugene, OR) was slowly injected into the left red nucleus (Coordinates: AP: 5.8 mm; ML: 0.7 mm; DV: 7.0 mm from Bregma) over 5 minutes using a 10  $\mu\text{l}$  Hamilton syringe. The needle was left in place for another 10 minutes and gradually

withdrawn over 3 minutes. Animals were allowed to survive for 2 weeks and were then sacrificed.

## Behavioral Testing

All behavioral tests were performed by individuals who were blinded with respect to treatment. All animals were tested preoperatively for their baseline performance on an open-field test, a test of forelimb usage, and a test of sensitivity to a thermal stimulus. Animals were tested for forelimb usage 3 days following the catheter implantation, before the funiculotomy, to check for deficits arising from the catheterization, and on forelimb usage, open-field, and thermal sensitivity tests at 1 week post-hemisection surgery, and then weekly for 8 weeks. At the end of the behavioral testing, a subset of animals was selected from each experimental group ( $n = 3$ ) for analysis of gait parameters using the CatWalk apparatus. Selection was based on an absence of history of autophagia, a common occurrence after certain spinal injuries in the rat, which damages the foot and thus perturbs gait. For each outcome measure of the footprint analysis, the variance among animals around the mean was low, resulting in a high degree of robustness and enough power to interpret the results. Gaits of the selected animals were compared to those of 7 unoperated controls.

**Forelimb Locomotor Scale Score**—The open-field locomotor (BBB) test<sup>33</sup> was developed to evaluate hindlimb function after midthoracic contusion injuries. Because the injury model in this experiment is a unilateral cervical lesion, we modified this test to assess open-field locomotion by the affected right fore-limb and hindlimb (Table 1). The forelimb scale was constructed to reflect the typical pattern of deficits and recovery. Rats were placed in an enclosure (1.5 × 0.6 meters) and videotaped for 4 minutes, and their performance was scored by 2 trained observers. Forelimb open-field scores range from 0 (*no function*) to 17 (*no deficit*).

**Forelimb Usage (Cylinder) Test**—The cylinder test is used to assess forelimb usage during exploration. Animals were placed into a Plexiglas cylinder (17.8 cm in diameter and 35.5 cm in height) and observed for 3 minutes. Normal animals spontaneously rear and explore, supporting themselves using one or both forelimbs placed against the wall. Injured animals may explore from a crouched position but still contact the wall of the cylinder with their forepaws. The number of fore-limb contacts is expressed as percentage of forelimb contacts with right plus both forepaws to total contacts.<sup>27,34</sup> This test is sensitive to lateral funiculus injury, and recovery is improved by therapeutic transplants.<sup>27,28</sup>

**Gait Analysis**—The CatWalk apparatus enabled us to measure several features of the dynamics of locomotion, including inter-limb coordination, limb base of support, and stride length.<sup>35,36</sup> The animals cross a walkway made of Plexiglas walls spaced 10.5 cm apart with a glass floor (122 × 15 × 1 cm), modified from Hamers et al.<sup>35</sup> Animals were filmed from the ventral perspective while they traversed the walkway, using a Pulnix TM 745E camera (Pulnix America, Inc, Sunnyvale, CA), equipped with a wide-angle objective (Cosimar 8.5 mm). Light from an encased white fluorescent tube (117 cm long) is reflected onto the glass floor. Paw contact with the floor interrupts the light and is recorded by the camera.<sup>37,38</sup> Data collection starts as the animal enters the walkway and stops as the animal exits. The signal is digitized (50 half-frames/sec) by a PCimage-SRGB frame grabber board (Matrix Vison GmbH, Openheimer, Germany). The CatWalk program<sup>35</sup> acquires, compresses, stores, and analyzes the gait parameters.

Data analysis was performed by interactively categorizing and labeling the signals (right/left fore/hind paw, nose, abdomen, tail, and artifact). The position, size, and intensity of these pixels were analyzed. Analysis is facilitated by using false colors for the display. The algorithm tracks

data between frames to provide automatic scoring. False positives (eg, fecal pellets) are also detected by the algorithm and can be manually edited. Each animal was tested 3 times, and each trial included at least 5 step cycles (producing 15–25 steps), which yielded a coefficient of variation sufficiently small to produce reliable data for this animal model. The following gait parameters were extracted from the CatWalk program<sup>35</sup>: *Regularity index* (RI) grades the degree of interlimb coordination by calculating the percentage of steps within a normal stepping pattern<sup>39</sup> divided by the total number of paw placements. Intact animals are fully coordinated with an RI of 100% (although it may appear slightly lower if incomplete step sequences are collected). Poor interlimb coordination is reflected by a lower RI. *Base of support* is measured by the perpendicular distance between 2 parallel lines crossing the center of the right and left paw paths. A wide base of support is consistent with impaired locomotor function. *Stride length* is the distance the right forelimb travels during a step cycle. We report this measure only for the affected right forelimb. *Swing duration* is the time during which the foot is not in contact with the surface. We report this measure only for the affected right forelimb. *Crossing time* is the time from the first paw placement to the last, recorded by the camera while the animal crosses the walkway.

**Thermal Sensitivity Test**—The thermal sensitivity test measures the latency of withdrawal of a limb in response to heat stimuli applied to the paw. Animals were placed in elevated Plexiglas cages for 30 minutes. A movable radiant heat source (25°C to 29°C) was applied to the left hindpaw or right forepaw and the time taken to withdraw noted. If a paw was not withdrawn after 30 seconds, the heat source was removed to prevent tissue damage. Five trials were run for each paw with a 15-minute interval between each trial to prevent sensitization.<sup>40–42</sup> Five trials were run for each paw. The last 4 trials were averaged to provide the mean latency of withdrawal.

**Data Analysis and Statistics: Behavior**—All weekly behavioral data were analyzed by 2-way ANOVA between groups (NEP1-40 treatment vs op-controls) and time, with time taken as a repeated measure. Post hoc analysis was performed, where appropriate, using the Bonferroni test. Operated control (n = 3) and NEP1-40 (n = 3) groups were compared to 7 normal rats for all gait parameters on the CatWalk by 1-way ANOVA to quantify deficits. Power analysis confirmed that interpretable data could be collected from this small sample. NEP 1-40 animals were compared to op-controls to assess treatment effects for each parameter using Student's *t* test. For other behavior tests, the NEP1-40 group was compared with op-control group and to preoperative baseline assessments. All data were analyzed by 2-way ANOVA between NEP1-40 treatment and time, with time taken as repeated measure. Significance levels were set to .05 for all comparisons.

## Histological Analysis

**Tissue Preparation**—Two weeks after BDA injection, rats were deeply anaesthetized with sodium pentobarbital (100 mg/kg; Abbott Laboratories, North Chicago, IL) and transcardially perfused with 200 mL normal saline followed by 500 mL of ice-cold 4% paraformaldehyde in 0.1 M phosphate buffer, pH 7.4. The spinal cord was removed and immersed in a 0.1 M phosphate buffer (PB) at 40°C, then in 30% sucrose (in 0.1 M PB containing 0.5 μM Thimerosal) for 3 to 5 days for cryoprotection. The spinal cord was serially blocked, embedded in OCT (Fisher Scientific, Pittsburgh, PA), cut into 20 μm longitudinal sections on a cryostat, and mounted onto gelatin-coated slides. Spinal cord sections were processed for BDA staining, Nissl-myelin, and immunohistochemistry with antibodies against 5-HT to identify raphe-spinal axons and calcitonin gene-related peptide (CGRP) to identify dorsal root axons. Nissl-myelin staining was performed on the cervical coronal sections 5 mm rostral to the lesion to evaluate catheter damage. Experimenters were blinded to the group identities of the animals.

**Lesion/Matrix**—Nissl myelin–stained sections through the lesion site were examined to determine that the lesion included the entire lateral funiculus and thus ablated the rubrospinal tract, and that the lesion site remained filled with the Vitrogen matrix.

**Evaluation of Catheter Damage**—Postmortem analysis indicated that the catheter produced variable damage to the spinal cord in all animals. Nissl myelin–stained sections through the area of catheter damage were examined by 2 independent investigators who identified areas of tissue damage for each animal. A ratio of the area of tissue loss to the normalized area of spinal cord was calculated for each animal. Two animals from the NEP1-40 group had dense scar formation or massive tissue damage caused by the catheter at sites other than the dorsal columns. These 2 animals were removed from the study.

**BDA Labeling**—Four animals with comparable and validated injections into the red nucleus were analyzed from each group. A 1 cm block of cervical spinal cord that included the lesion site was sectioned longitudinally at 20  $\mu$ m. BDA-labeled fibers were detected by staining with an ABC (avidin-biotin-peroxidase complex) elite kit (Vector, Burlingame, CA), using the protocols described by Liu.<sup>27</sup> Slides were rinsed 3 times for 30 minutes each with TBST (50 mM Tris-buffered saline containing 0.5% Triton X-100, pH 10.0) and then incubated overnight with an ABC elite kit at 4°C. On the second day, after four 30-minute rinses in TBST and a 5-minute rinse in 50 mM Tris buffer at pH 10 and pH 7.2 each, the sections were reacted with Sigma Fast–DAB compounds (Sigma, St Louis, MO). Sections were counterstained with cresyl violet, dehydrated, and coverslipped with DPX (Fluka Chemie AG, Buchs, Switzerland).

The number of BDA-labeled fibers rostral to, at the lesion epicenter, and caudal to the lesion in both white and gray matter and both ipsilateral and contralateral to the lesion site was analyzed using a light microscope with bright-field illumination at a final magnification of  $\times 20$ . Sections were selected at 200- $\mu$ m intervals, and the fibers were counted on 3 planes that crossed the rostral edge, epicenter, and caudal edge of the lesion. Because the efficiency of BDA labeling varies from animal to animal, we quantified the BDA labeling 5 mm rostral to the lesion epicenter to provide a normalization control; because axotomized rubrospinal axons retract after axotomy a distance of  $\sim 500$   $\mu$ m,<sup>43</sup> axons 5 mm rostral to the injury should reflect surviving rubrospinal axons. The total number of BDA-labeled fibers in the vicinity of the lesion site was divided by the total number of the fibers 5 mm rostral to the lesion to provide comparable densities.<sup>27</sup>

**Immunohistochemistry**—Spinal cord sections were processed for immunohistochemistry with antibodies against serotonin to identify raphe-spinal axons and CGRP to identify peptidergic dorsal root axons. The sections were washed 3 times in PBS for 5 minutes each, incubated in PBS that contains 10% normal goat serum (NGS) for 1 hour at room temperature, and then incubated in 2% NGS + polyclonal serotonin (1:20,000; Immunostar, Hudson, WI) or polyclonal CGRP (1:4,000; Peninsula Laboratories, Belmont, CA) in PBS overnight at 4°C in a humidified chamber. Sections were washed with PBS 3 times the following day, incubated with fluorescently conjugated rhodamine-conjugated goat antirabbit (1:200; Jackson ImmunoResearch, West Grove, PA) in PBS for 2 hours at room temperature, washed with PBS, and then coverslipped with vectashield that contains the nuclear counterstain DAPI (Vector, San Diego, CA). Stained sections were examined with a Leica DMRBE microscope (Wetzlar, Germany), and images were captured by using Reteiga Exi camera (QImaging Corp, Burnaby, BC, Canada). Images were processed on a PC computer with an imageJ program. The images of the lesion site and surrounding tissue were captured within a fixed box size of 1360  $\times$  1036 pixels at 10 $\times$  for 5 HT and CGRP immunoreactivity. Threshold values were set so only immunoreactive axons were measured. Nonspecific staining, such as obvious artifacts caused by tissue processing, was edited from images. Total labeled axons were measured as area fraction.

**Statistics: Tissue Analysis**—To analyze BDA-labeled axons, area of catheter damage, and quantification of immunohistochemistry, NEP1-40-treated animals were compared to op-controls by 1-way ANOVA. A regression test was used to analyze the correlation between severity of catheter damage and average score on the cylinder test at 5 to 8 weeks. Significance levels were set to .05 for all comparisons.

## RESULTS

### Behavioral Analysis

**Forelimb Locomotor Scale Score**—Intact animals have forelimb locomotor scale scores of 17. One week after the lateral funiculotomy, forelimb open field scores in both groups showed a modest but significant ( $P < .05$ ) deficit followed by a recovery that plateaued at week 2, with no differences between groups (Figure 1). Thus, this test was sensitive enough to reveal an early deficit following the spinal lesion, the NEP1-40 treatment did not protect against this deficit, and animals in both groups recovered equally well.

**Forelimb Exploration**—Intact rats support themselves on their hindlimbs and explore the walls of the cylinder using their fore-limbs; about 25% of contacts are made with the right, 25% with the left, and 50% with both forepaws. In normal animals, the right forelimb is therefore used in about 75% of all contacts. Both op-control and NEP1-40 groups showed normal frequencies of contacts during baseline testing and 3 days after the catheter implantation. Decreased use of the right forelimb was evident in both groups by 1 week after the lateral funiculotomy. The op-control group showed no further recovery during the experimental period. The NEP1-40, in contrast, showed significantly ( $P < .05$ ) greater recovery at weeks 2 through 7, although the right forelimb usage declined at week 8 to the level of the op-control group (Figure 2). Thus, the improvement in the NEP1-40 group may not have been permanent.

**Gait Analysis**—ANOVA revealed significant differences between the operated groups for gait parameters collected using the CatWalk apparatus. Gait parameters were then compared between normal animals and the 3 representatives of the op-control and NEP1-40-treated groups at the end of the study, 8 weeks postinjury. The animals for CatWalk analysis were chosen because they had no history of autophagy and their forepaws were intact. These animals performed similarly to the group means on the other behavioral tests, and their selection does not represent a bias. Steps made by NEP1-40-treated animals were very similar to those made by normal rats (Figure 3). The following gait analysis parameters were extracted from at least 15 of these step cycles. The right forelimb stride length (Figure 4A), RI (Figure 4B), fore-limb and hindlimb base of support (Figure 4C, D), crossing time (Figure 4E), and swing duration (Figure 4F) of the right forelimb were all similar to normal values. In contrast, gait parameters were significantly impaired in the op-control group. The right forelimb stride length was reduced ( $P < .05$ , Figure 4A). The RI was also reduced, indicating poor interlimb coordination ( $P < .05$ , Figure 4B). Although the forelimb base of support was similar to that of intact rats (Figure 4C), the hindlimb base of support was increased ( $P < .05$ ), indicating a broader-based gait (Figure 4D). Crossing time was also longer ( $P < .05$ , Figure 4E) and swing duration of the right forelimb greater ( $P < .05$ , Figure 4F), indicating a right forelimb deficit. By dividing stride length by swing duration, we calculated the swing velocity of the limb. This measure confirms that the op-controls exhibit impaired use of their forelimb whereas the NEP1-40-treated animals behave similar to normals. Gait parameters of the other limbs were also altered, suggesting that the animals are compensating for these deficits (data not shown), but because of individual variation in compensatory responses, these parameters could not be further analyzed within our limited sample. Thus, gait analysis was a sensitive indicator of deficits in

the op-control group and showed that NEP1-40 treatment appears to have largely eliminated gait deficits.

**Thermal Sensitivity**—The heat test measures the latency of limb withdrawal in response to thermal stimuli applied to the ventral surface of the paw and is thus a measure of sensorimotor function. Reductions in withdrawal latency denote hypersensitivity to heat stimuli. Right-sided lesions of the lateral funiculus damage the region around the ipsilateral dorsal root entry zone, including sensory fibers representing the ipsilateral forelimb and the spinothalamic tract, which contains ascending axons relaying information from the contralateral side. Therefore we expect any deficits in sensory processing to be most severe in the right forelimb and the left hindlimb.<sup>34</sup>

Technical difficulties that occurred at week 1 precluded data collection for that time point. The operated controls showed decreased latency of withdrawal in both right forelimb and left hindlimb when tested at week 2 ( $P < .05$ ), compared to baseline, but recovered to baseline latency thereafter. Latency of withdrawal did not change from baseline levels postoperatively in the NEP1-40 group. Thus, the NEP1-40 treatment did not induce thermal hypersensitivity, whereas the op-controls showed early hypersensitivity but only transiently (Figure 5).

### Histological Analysis

**Lesion/Matrix Site**—In all cases, the lesion ablated the lateral funiculus and thus severed the rubrospinal tract (data not shown). The lesion cavity contained the Vitrogen matrix, some host cells that had migrated into the matrix, and some axons (see below) that had grown into the matrix. Thus, the matrix persisted and filled the lesion cavity, providing a permissive substrate for axonal growth, as shown previously.<sup>31,32</sup>

**Catheter Site**—The cervical spinal cord sections showed tissue damage from the catheter in all animals. Thus, the NEP1-40 or vehicle had access to the parenchyma in all experimental animals. One animal had extensive glial scar formation that extended to the dorsal horn, and in another the ventral horn and ventral and lateral funiculi were damaged (Figure 6). The data from these 2 animals, both from the NEP1-40 group, were removed from the behavioral analyses, reducing the number of NEP1-40 animals to 6. To determine whether the catheter damage was correlated with behavioral deficits in the other animals, we compared percent of tissue damage associated with the catheter with scores on the test of forelimb function (Table 2). The catheter damage was calculated as the area of tissue loss divided by the area of normal spinal cord in cross section. The percent damage did not differ between the 7 op-control and 6 NEP1-40-treated rats. Because the score on the cylinder test had plateaued by 5 weeks postinjury, we averaged the scores from the forelimb test from week 5 to week 8. There was no correlation between damage and behavioral performance ( $R^2 = 0.0$ ) in the groups that were tested in the open field, exploration, or thermal sensitivity tests or in the subset that was tested on the CatWalk.

**BDA Anterograde Tracing**—The injection of BDA into the red nucleus (Figure 7C, D) labels rubrospinal axons. To analyze the effect of NEP1-40 treatment on rubrospinal axons, we examined the BDA-labeled axons at the epicenter, rostral edge, and caudal edge of the lesion in longitudinal sections (Figure 7A, B) and quantified labeled axons in both gray matter and lateral funiculus ipsilateral and contralateral to the injury (Figure 8). Because the efficiency of BDA labeling varied from animal to animal, a horizontal plane 5 mm rostral to the epicenter of the lesion was chosen as an internal normalization control. The number of BDA-labeled axons obtained from each region was divided by the total number of BDA-labeled axons obtained at 5 mm rostral to the lesion epicenter and expressed as a percentage of normal density.



In normal control animals, the BDA-labeled rubrospinal axons appear as a bundle of fibers with a straight trajectory localized to the right lateral funiculus. A small number of axons were present in the same location in the contralateral lateral funiculus, representing the 1% of RST fibers that are uncrossed (data not shown). In the NEP1-40-treated group, compared to the op-controls, significantly ( $P < .05$ ) more BDA-labeled axons reached the rostral edge of the lesion/matrix, although few or none entered the lesion/matrix site (Figure 8A). BDA axons were present in the contralateral gray matter in both groups, but more BDA axons were seen in the contralateral gray matter in the NEP1-40 group ( $P < .05$ , Figure 8D), suggesting enhanced sprouting from lesioned ipsilateral axons across the midline or from uninjured contralateral axons. At the caudal edge of the lesion/matrix site, there was no difference between groups in number of BDA-labeled axons (Figure 8A, C). Thus, NEP1-40 increased regeneration and/or sprouting and/or decreased dieback of injured RST axons. BDA-labeled axons, however, did not enter the lesion/matrix site nor did they extend in gray or white matter caudal to the lesion/matrix site.

### Immunohistochemical Analysis

**Serotonergic Axons**—In the NEP1-40 treated group, serotonin-immunoreactive fibers were present within the Vitrogen-filled lesion cavity. These fibers were distributed mostly in the rostral half and the center of the lesion, but some extended beyond the center and toward the caudal end of the matrix-filled cavity. Robust 5 HT staining was seen in the host gray matter and white matter adjacent to the graft. Fibers entered the lesion/matrix from the host gray matter or ipsilateral lateral funiculus (Figure 9A, B, C). In the op-control group, very few serotonin-immunoreactive fibers were found around or in the Vitrogen-filled lesion site (Figure 9D, E, F). Quantification of the area fraction of the immunoreaction within the matrix/lesion indicated denser ( $P < .05$ ) staining in the NEP1-40 group compared to the op-controls (Figure 11A).

**Peptidergic Axons**—Dorsal root axons containing CGRP were observed within the lesion/matrix in both groups (Figure 10), but NEP1-40-treated animals (Figure 10A, B, C) contained denser CGRP staining ( $P < .05$ ; Figure 11B) than the op-control group (Figure 10D, E, F).

NEP1-40 treatment therefore promoted growth or sprouting of raphe-spinal and peptidergic dorsal root fibers into the matrix-filled lesion site. The failure of BDA-labeled rubrospinal axons to enter the lesion/matrix site is therefore not due to an impenetrable barrier but perhaps to a less robust capacity for growth by RST axons.

## DISCUSSION

We show that several gait parameters return to nearly normal levels and that usage of the forelimb ipsilateral to the injury is greater in NEP1-40 recipients. Neither the lesion nor the NEP1-40 infusion produced prolonged hypersensitivity to a thermal stimulus. Administration of NEP1-40 is expected to diminish the inhibitory environment of the CNS, which could foster random growth of axons that could disrupt function. In no case did NEP1-40 treatment impair recovery. NEP1-40 treatment diminished rubrospinal axonal dieback and/or increased axon sprouting or regeneration in white matter and also into gray matter rostral to and at the level of but not caudal to the lesion. Descending serotonergic and CGRP-containing primary afferent axons showed increased growth adjacent to and into the lesion/matrix site in NEP1-40 recipients. Thus, efficacy of NEP1-40 in promoting recovery of function and repair is thus shown in a second spinal injury model. NEP1-40 appeared, however, to be less effective in stimulating regeneration of rubrospinal axons caudal to the injury compared to the lesioned corticospinal tract in animals treated with Nogo A antibody.<sup>11,44,45</sup> NEP1-40 was also not as effective as transplants of fibroblasts genetically modified to express brain-derived neurotrophic factor (BDNF) or olfactory glia or AAV delivery of trophic factors, which induced

regeneration of rubrospinal axons through, around, and distal to the transplant<sup>27,28,46</sup> in the same lesion model.

## Recovery of Function

**Gait Analysis**—Gait analysis using the CatWalk was a more sensitive test of motor function following a lateral funiculotomy than the Forelimb Locomotor Scale Score. Efficient and integrated locomotion is largely dependent on the descending pathways in the ventromedial and ventrolateral funiculi, which were spared in the operated animals.<sup>47,48</sup> Animals in the op-control group were able to locomote but showed dysfunction of right forelimb, lack of interlimb coordination, and compensatory modifications in left forelimb function. In contrast, all measured gait parameters in NEP1-40-treated animals recovered to nearly normal levels. Given the lack of long-distance growth of rubrospinal axons, which we believe reflects lack of long-distance growth of other descending pathways, the nearly normal function implies that local plasticity induced by the NEP1-40 treatment is sufficient to provide recovery of coordinated hindlimb and forelimb function and that the improved function is apparent 2 months after the injury and 1 month following cessation of NEP1-40 administration.

**Forelimb Usage**—The recovery of forelimb usage, as seen in the cylinder test, showed an improvement in the NEP1-40 group, compared to the op-controls, although right forelimb usage declined at the end of the experiment. It is possible that the absence of NEP1-40 infusion in the last 4 weeks of the study led to the decreased function. We do not know when the additional damage to axons caused by the catheter occurred, but this could also have contributed to the decrease in forelimb exploratory function seen at 8 weeks. Although our catheterization procedure was similar to that used by GrandPré et al,<sup>11</sup> their catheters were placed above the injury site (dorsal hemisection) in the thoracic spinal cord, whereas we inserted the catheter into the much narrower space in the cervical spinal canal, which presumably accounted for the additional damage to the dorsal columns. The catheter damage was, however, similar in the 2 groups that we tested and did not prevent the demonstration of overall greater functional recovery provided by the NEP1-40 treatment in this test.

**Thermal Sensitivity**—Because contusion and hemisection<sup>34,49–51</sup> injuries have induced hypersensitivity to thermal stimuli applied to the hindlimb, we tested whether the more restricted lesion that we used would also increase sensitivity. We found increased sensitivity compared to baseline only in the op-control group and only at 2 weeks. Both experimental groups were at baseline levels thereafter with no differences between the groups, indicating that neither the lateral funiculotomy nor the NEP1-40 treatment induced hindlimb hypersensitivity.

## Axonal Growth

Anterograde labeling of specific motor pathways can provide evidence that the intervention stimulates regenerative growth. GrandPré and colleagues<sup>11</sup> reported that NEP1-40 administration to rats with dorsal hemisections induced sprouting by injured corticospinal axons at the rostral edge of the lesion and that some injured axons regenerated through intact ventral corticospinal tract caudal to the lesion and some regenerated considerable distances. Similarly, NgR treatment after midthoracic contusion enhances corticospinal sprouting rostral to and raphe-spinal sprouting caudal to the contusion.<sup>52</sup> Primate studies have described that NgR neutralization following cervical lateral funiculus lesions also promotes corticospinal sprouting rostral to and regeneration caudal to a spinal injury.<sup>45,53</sup> We show that NEP1-40 treatment preserves rubrospinal axons at the rostral edge of the lesion by preventing dieback and/or by eliciting regenerative sprouting. Some labeled axons entered the gray matter and possessed varicosities with morphology consistent with synaptic boutons (data not shown). There was, however, no difference between the groups in the density of rubrospinal tract

staining caudal to the lesion. Thus, growth or failure of dieback by RST axons, stimulated by NEP1-40, was more limited than that reported for the CST or for that elicited by genetically modified fibroblasts in a similar model.<sup>27,28</sup>

Sprouting (or regeneration) by raphe-spinal and dorsal root axons occurs following a number of experimental interventions, including various kinds of grafts and modifications of the environment.<sup>54–60</sup> Nogo blockade increases raphe-spinal sprouting caudal to a contusion injury<sup>52</sup> and after dorsal hemisection.<sup>61</sup> We show that NEP1-40 increases growth of host raphe-spinal and also dorsal root axons into and adjacent to the lesion/matrix. The serotonergic and dorsal root axons in the NEP1-40 group, unlike BDA-labeled rubrospinal axons, entered the lesion/matrix site. Thus, the lesion/matrix boundary did not preclude entry of axons. Serotonergic and dorsal root axons may be more successful at extending axons than the rubrospinal axons, which showed no tendency to grow into the matrix. Thus, injured rubrospinal axons may respond less robustly to NEP1-40 administration than serotonergic and dorsal root axons<sup>56</sup> or corticospinal axons.<sup>11</sup>

The axonal growth elicited by NEP1-40 administration is likely due primarily to the blockade of a set of inhibitory molecules that are normally present in the spinal cord. Interestingly, these inhibitors require binding to coreceptors, one of which is the p75 receptor, to be effective. Neurotrophic factors also bind to the p75,<sup>17</sup> which suggests that a competition for binding to this coreceptor may influence how permissive or inhibitory the environment is to axonal growth.<sup>58,60</sup> Thus, blockade of the inhibitors may act to increase the efficacy of neurotrophins that may be present and could increase the likelihood of sprouting by damaged (rubrospinal or raphe-spinal) or intact (dorsal root) systems.

### Receptor Blockade Versus Nogo Knockouts

Although treatments that neutralize Nogo-A or NgR elicit increased axonal growth in this study and others,<sup>11,22–26,44,62–64</sup> studies using Nogo or NgR knockout mice have reported much less consistent axonal growth following SCI.<sup>65–69</sup> These varying degrees of axonal growth in the Nogo knockout mice appear to be related to the different genetic backgrounds of the mice used in these studies.<sup>62,70,71</sup> It is also possible that IN-1 or NEP1-40 may have direct regenerative effects, which would contribute to the more robust growth.<sup>72</sup> For example, IN-1 treatment up-regulates the level of BDNF, vascular endothelial growth factor, and growth-associated protein 43.<sup>73</sup> Therefore, the absence of Nogo in the knockout mice may further impair the ability of neurons to respond to SCI.

## CONCLUSIONS

This study demonstrates that NEP1-40 prevents dieback and/or promotes growth of rubrospinal axons into gray matter and stimulates dorsal root and serotonergic axonal growth in the vicinity of and into the lesion/matrix site and promotes functional recovery. The recovery is likely due to changes in the local circuitry that engage host interneuronal systems. Our results also suggest that severed rubrospinal axons respond to the NEP1-40 treatment less robustly than the dorsal corticospinal, raphe-spinal, or dorsal root axons<sup>11,56</sup> or to transplants of fibroblasts genetically modified to secrete neurotrophins<sup>27</sup> or to transplants of olfactory cells.<sup>28</sup>

## Acknowledgments

We thank Dr Tony Yaksh and Dr Jane Relton for their invaluable advice. Supported by NS24707, Biogen-IDEC, Inc, and T32HD07467.

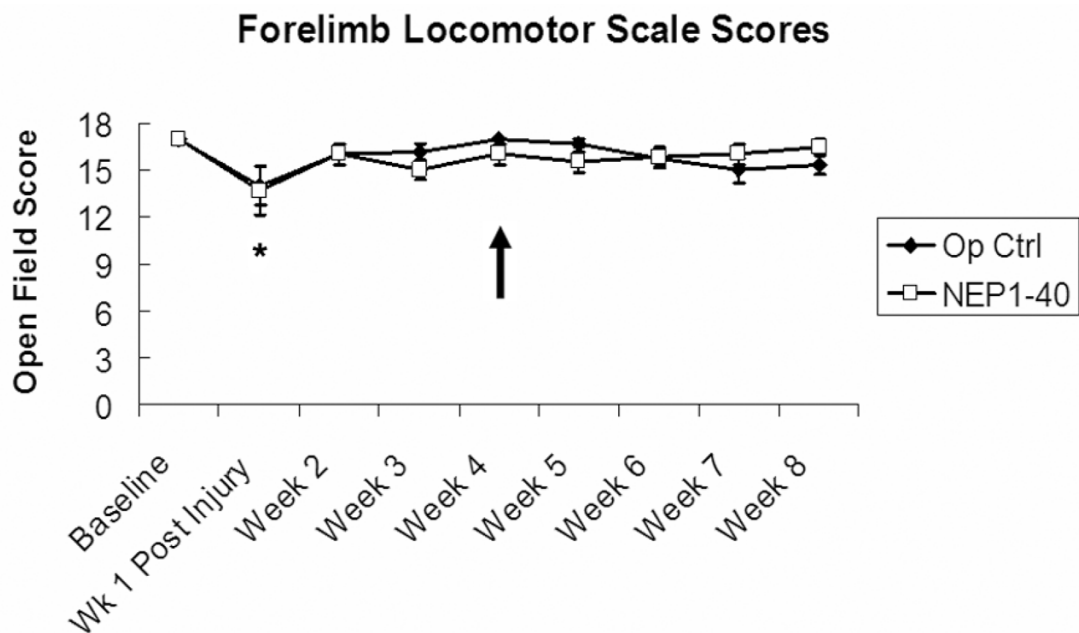
## References

1. Hunt D, Coffin RS, Anderson PN. The Nogo receptor, its ligands and axonal regeneration in the spinal cord; a review. *J Neurocytol* 2002;31:93–120. [PubMed: 12815233]
2. Savio T, Schwab ME. Lesioned corticospinal tract axons regenerate in myelin-free rat spinal cord. *Proc Natl Acad Sci U S A* 1990;87:4130–4133. [PubMed: 2349222]
3. Chen MS, Huber AB, van der Haar ME, et al. Nogo-A is a myelin-associated neurite outgrowth inhibitor and an antigen for monoclonal antibody IN-1. *Nature* 2000;403:434–439. [PubMed: 10667796]
4. Prinjha R, Moore SE, Vinson M, et al. Inhibitor of neurite outgrowth in humans. *Nature* 2000;403:383–384. [PubMed: 10667780]
5. Oertle T, van der Haar ME, Bandtlow CE, et al. Nogo-A inhibits neurite outgrowth and cell spreading with three discrete regions. *J Neurosci* 2003;23:5393–5406. [PubMed: 12843238]
6. McKerracher L, David S, Jackson DL, et al. Identification of myelin-associated glycoprotein as a major myelin-derived inhibitor of neurite growth. *Neuron* 1994;13:805–811. [PubMed: 7524558]
7. Mukhopadhyay G, Doherty P, Walsh FS, et al. A novel role for myelin-associated glycoprotein as an inhibitor of axonal regeneration. *Neuron* 1994;13:757–767. [PubMed: 7522484]
8. Kottis V, Thibault P, Mikol D, et al. Oligodendrocyte-myelin glycoprotein (OMgp) is an inhibitor of neurite outgrowth. *J Neurochem* 2002;82:1566–1569. [PubMed: 12354307]
9. Wong ST, Henley JR, Kanning KC, et al. A p75(NTR) and Nogo receptor complex mediates repulsive signaling by myelin-associated glycoprotein. *Nat Neurosci* 2002;5:1302–1308. [PubMed: 12426574]
10. GrandPré T, Nakamura F, Vartanian T, et al. Identification of the Nogo inhibitor of axon regeneration as a Reticulon protein. *Nature* 2000;403:439–444. [PubMed: 10667797]
11. GrandPré T, Li S, Strittmatter SM. Nogo-66 receptor antagonist peptide promotes axonal regeneration. *Nature* 2002;417:547–551. [PubMed: 12037567]
12. Fournier AE, GrandPré T, Strittmatter SM. Identification of a receptor mediating Nogo-66 inhibition of axonal regeneration. *Nature* 2001;409:341–346. [PubMed: 11201742]
13. Domeniconi M, Cao Z, Spencer T, et al. Myelin-associated glycoprotein interacts with the nog066 receptor to inhibit neurite outgrowth. *Neuron* 2002;35:283–290. [PubMed: 12160746]
14. Liu BP, Fournier A, GrandPré T, et al. Myelin-associated glycoprotein as a functional ligand for the nogo-66 receptor. *Science* 2002;297:1190–1193. [PubMed: 12089450]
15. Wang KC, Koprivica V, Kim JA, et al. Oligodendrocyte-myelin glycoprotein is a Nogo receptor ligand that inhibits neurite outgrowth. *Nature* 2002;417:941–944. [PubMed: 12068310]
16. Wang KC, Kim JA, Sivasankaran R, et al. P75 interacts with the Nogo receptor as a co-receptor for Nogo, MAG and OMgp. *Nature* 2002;420:74–78. [PubMed: 12422217]
17. McGee AW, Strittmatter SM. The Nogo-66 receptor: focusing myelin inhibition of axon regeneration. *Trends Neurosci* 2003;26:193–198. [PubMed: 12689770]
18. Mi S. LINGO-1 is a component of the Nogo-66 receptor/p75 signaling complex. *Nat Neurosci* 2004;7:221–228. [PubMed: 14966521]
19. Park JB, Yiu G, Kaneko S, et al. A TNF receptor family member, TROY, is a coreceptor with Nogo receptor in mediating the inhibitory activity of myelin inhibitors. *Neuron* 2005;45:345–351. Erratum in: *Neuron*. 2005;45:815. [PubMed: 15694321]
20. Shao Z, Browning JL, Lee X, et al. TAJ/TROY, an orphan TNF receptor family member, binds Nogo-66 receptor 1 and regulates axonal regeneration. *Neuron* 2005;45:353–359. [PubMed: 15694322]
21. Schnell L, Schwab ME. Axonal regeneration in the rat spinal cord produced by an antibody against myelin-associated neurite growth inhibitors. *Nature* 1990;343:269–272. [PubMed: 2300171]
22. Bregman BS, Kunkel-Bagden E, Schnell L, et al. Recovery from spinal cord injury mediated by antibodies to neurite growth inhibitors. *Nature* 1995;378:498–501. [PubMed: 7477407]
23. Brösamle C, Huber AB, Fiedler M, et al. Regeneration of lesioned corticospinal tract fibers in the adult rat induced by a recombinant, humanized IN-1 antibody fragment. *J Neurosci* 2000;20:8061–8068. [PubMed: 11050127]
24. Li S, Strittmatter SM. Delayed systemic Nogo-66 receptor antagonist promotes recovery from spinal cord injury. *J Neurosci* 2003;23:4219–4227. [PubMed: 12764110]

25. Li S, Liu BP, Budel S, et al. Blockade of Nogo-66, myelin-associated glycoprotein, and oligodendrocyte myelin glycoprotein by soluble Nogo-66 receptor promotes axonal sprouting and recovery after spinal injury. *J Neurosci* 2004;24:10511–10520. [PubMed: 15548666]
26. Ji B, Li M, Budel S, et al. Effect of combined treatment with methyl-prednisolone and soluble Nogo-66 receptor after rat spinal cord injury. *Eur J Neurosci* 2005;22:587–594. [PubMed: 16101740]
27. Liu Y, Kim D, Himes BT, et al. Transplants of fibroblasts genetically modified to express BDNF promote regeneration of adult rat rubrospinal axons and recovery of forelimb function. *J Neurosci* 1999;19:4370–4387. [PubMed: 10341240]
28. Xiao M, Klueber KM, Lu C, et al. Human adult olfactory neural progenitors rescue axotomized rodent rubrospinal neurons and promote functional recovery. *Exp Neurol* 2005;194:12–30. [PubMed: 15899240]
29. Yaksh TL, Rudy TA. Chronic catheterization of the spinal sub-arachnoid space. *Physiol Behav* 1976;17:1031–1036. [PubMed: 14677603]
30. Jones LL, Tuszynski MH. Chronic intrathecal infusions after spinal cord injury cause scarring and compression. *Microscopy Res Technique* 2001;54:317–324.
31. Hayashi Y, Shumsky JS, Connors T, et al. Immunosuppression with either cyclosporine A or FK506 supports survival of transplanted fibroblasts and promotes growth of host axons into the transplant after spinal cord injury. *J Neurotrauma* 2005;22:1267–1281. [PubMed: 16305315]
32. Nothias J-M, Mitsui T, Shumsky JS, et al. Combined effects of neurotrophin secreting transplants, exercise, and serotonergic drug challenge improve function in spinal rats. *Neurorehabil Neural Repair* 2005;19:296–312. [PubMed: 16263962]
33. Basso DM, Beattie MS, Bresnahan JC. A sensitive and reliable locomotor rating scale for open field testing in rats. *J Neurotrauma* 1995;12:1–21. [PubMed: 7783230]
34. Shumsky JS, Tobias CA, Tumolo M, et al. Delayed transplantation of fibroblasts genetically modified to secrete BDNF and NT-3 into a spinal cord injury site is associated with limited recovery of function. *Exp Neurol* 2003;184:114–130. [PubMed: 14637085]
35. Hamers FP, Lankhorst AJ, van Laar TJ, et al. Automated quantitative gait analysis during overground locomotion in the rat: its application to spinal cord contusion and transection injuries. *J Neurotrauma* 2001;18:187–201. [PubMed: 11229711]
36. Vrinten DH, Hamers FPT. ‘CatWalk’ automated quantitative gait analysis as a novel method to assess mechanical allodynia in the rat; a comparison with von Frey testing. *Pain* 2003;102:203–209. [PubMed: 12620612]
37. Betts RP, Duckworth T. A device for measuring plantar pressures under the sole of the foot. *Eng Med* 1978;7:223–228.
38. Clarke KA. A technique for the study of spatiotemporal aspects of paw contact patterns, applied to rats treated with a TRH analogue. *Beh Res Methods Instr Comp* 1992;24:407–411.
39. Cheng H, Almstrom S, Gimenez-Llort L, et al. Gait analysis of adult paraplegic rats after spinal cord repair. *Exp Neurol* 1997;148:544–557. [PubMed: 9417831]
40. Eliav E, Herzberg U, Ruda MA, et al. Neuropathic pain from an experimental neuritis of the rat sciatic nerve. *Pain* 1999;83:169–182. [PubMed: 10534588]
41. Hargreaves K, Dubner R, Brown F, et al. A new and sensitive method for measuring thermal nociception in cutaneous hyper-algesia. *Pain* 1988;32:77–88. [PubMed: 3340425]
42. Yeziarski RP, Liu S, Ruenes GL, et al. Excitotoxic spinal cord injury: behavioral and morphological characteristics of a central pain model. *Pain* 1998;75:141–155. [PubMed: 9539683]
43. Houle JD, Jin Y. Chronically injured supraspinal neurons exhibit only modest axonal dieback in response to a cervical hemisection lesion. *Exp Neurol* 2001;169:208–217. [PubMed: 11312573]
44. Liebscher T, Schnell L, Schnell D, et al. Nogo-A antibody improves regeneration and locomotion of spinal cord-injured rats. *Ann Neurol* 2005;58:706–719. [PubMed: 16173073]
45. Freund P, Schmidlin E, Wannier T, et al. Nogo-A-specific antibody treatment enhances sprouting and functional recovery after cervical lesion in adult primates. *Nat Med* 2006;12(7):790–792. [PubMed: 16819551]
46. Ruitenber MJ, Plant GW, Hamers FPT, et al. Ex vivo adenoviral vector-mediated neurotrophin gene transfer to olfactory ensheathing glia: effects on rubrospinal tract regeneration, lesion size, and

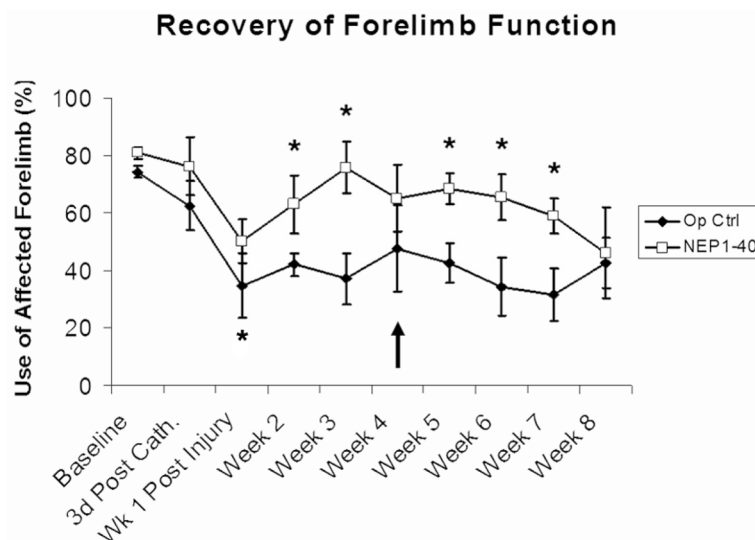
- functional recovery after implantation in the injured rat spinal cord. *J Neurosci* 2003;23:7045–7058. [PubMed: 12904465]
47. Steeves JD, Jordan LM. Localization of a descending pathway in the spinal cord which is necessary for controlled treadmill locomotion. *Neurosci Lett* 1980;20:283–288. [PubMed: 7443078]
  48. Bem T, Gorska T, Majczynski H, et al. Different patterns of fore-hindlimb coordination during overground locomotion in cats with ventral and lateral spinal lesions. *Exp Brain Res* 1995;104:70–80. [PubMed: 7621942]
  49. Christensen MD, Everhart AW, Pickelman JT, et al. Mechanical and thermal allodynia in chronic central pain following spinal cord injury. *Pain* 1996;68:97–107. [PubMed: 9252004]
  50. Christensen MD, Hulsebosch CE. Chronic central pain after spinal cord injury. *J Neurotrauma* 1997;14:517–537. [PubMed: 9300563]
  51. Hains BC, Chastain KM, Everhart AW, McAdoo DJ, et al. Transplants of adrenal medullary chromaffin cells reduce fore-limb and hindlimb allodynia in a rodent model of chronic central pain after spinal cord hemisection injury. *Exp Neurol* 2000;164:426–437. [PubMed: 10915581]
  52. Wang X, Baughman KW, Basso DM, et al. Delayed Nogo receptor therapy improves recovery from spinal cord contusion. *Ann Neurol* 2006;60(5):540–549. [PubMed: 16958113]
  53. Freund P, Wannier T, Schmidlin E, Bloch J, et al. Anti-Nogo-A antibody treatment enhances sprouting of corticospinal axons rostral to a unilateral cervical spinal cord lesion in adult macaque monkey. *J Comp Neurol* 2007;502(4):644–659. [PubMed: 17394135]
  54. Romero MI, Rangappa N, Garry MG, et al. Functional regeneration of chronically injured sensory afferents into adult spinal cord after neurotrophin gene therapy. *J Neurosci* 2001;21:8408–8416. [PubMed: 11606629]
  55. Tobias CA, Shumsky JS, Shibata M, et al. Delayed grafting of BDNF and NT-3 producing fibroblasts into the injured spinal cord stimulates sprouting, partially rescues axotomized red nucleus neurons from loss and atrophy, and provides limited regeneration. *Exp Neurol* 2003;184:97–113. [PubMed: 14637084]
  56. Ramer LM, Au E, Richter MW, et al. Peripheral olfactory ensheathing cells reduce scar and cavity formation and promote regeneration after spinal cord injury. *J Comp Neurol* 2004;473:1–15. [PubMed: 15067714]
  57. Hagg T, Baker KA, Emsley JG, et al. Prolonged local neurotrophin-3 infusion reduces ipsilateral collateral sprouting of spared corticospinal axons in adult rats. *Neuroscience* 2005;130:875–887. [PubMed: 15652986]
  58. Scott AL, Borisoff JF, Ramer MS. Deafferentation and neurotrophin-mediated intraspinal sprouting: a central role for the p75 neurotrophin receptor. *Eur J Neurosci* 2005;21:81–92. [PubMed: 15654845]
  59. Grider MH, Mamounas LA, Le W, et al. In situ expression of brain-derived neurotrophic factor or neurotrophin-3 promotes sprouting of cortical serotonergic axons following a neurotoxic lesion. *J Neurosci Res* 2005;82:404–412. [PubMed: 16206279]
  60. Schwab ME. Nogo and axon regeneration. *Curr Opin Neurobiol* 2004;14:118–124. [PubMed: 15018947]
  61. Cafferty WB, Strittmatter SM. The Nogo-Nogo receptor pathway limits a spectrum of adult CNS axonal growth. *J Neurosci* 2006;26(47):12242–12250. [PubMed: 17122049]
  62. Schnell, L.; Liebscher, T.; Weinmann, O., et al. Program no. 43.11. 2004 Abstract Viewer/Itinerary Planner. Washington, DC: Society for Neuroscience; Increased regeneration and functional recovery in rats treated with antibodies to Nogo-A and in Nogo-A knockout mice.
  63. Buchli AD, Schwab ME. Inhibition of Nogo: a key strategy to increase regeneration, plasticity and functional recovery of the lesioned central nervous system. *Ann Med* 2005;37(8):556–567. [PubMed: 16338758]
  64. Liu BP, Cafferty WB, Budel SO, et al. Extracellular regulators of axonal growth in the adult central nervous system. *Philos Trans R Soc Lond B Biol Sci* 2006;361(1473):1593–1610. [PubMed: 16939977]
  65. Simonen M, Pedersen V, Weinmann O, et al. Systemic deletion of the myelin-associated outgrowth inhibitor Nogo-A improves regenerative and plastic responses after spinal cord injury. *Neuron* 2003;38:201–211. [PubMed: 12718855]

66. Kim JE, Li S, GrandPré T, et al. Axon regeneration in young adult mice lacking Nogo-A/B. *Neuron* 2003;38:187–199. [PubMed: 12718854]
67. Zheng B, Ho C, Li S, et al. Lack of enhanced spinal regeneration in Nogo-deficient mice. *Neuron* 2003;38:213–224. [PubMed: 12718856]
68. Kim JE, Liu BP, Park JH, et al. Nogo-66 receptor prevents raphespinal and rubrospinal axon regeneration and limits functional recovery from spinal cord injury. *Neuron* 2004;44:439–451. [PubMed: 15504325]
69. Zheng B, Atwal J, Ho C, et al. Genetic deletion of the Nogo receptor does not reduce neurite inhibition in vitro or promote corticospinal tract regeneration in vivo. *Proc Natl Acad Sci U S A* 2005;102:1205–1210. [PubMed: 15647357]
70. Dimou L, Schnell L, Montani L, et al. Nogo-A-deficient mice reveal strain-dependent differences in axonal regeneration. *J Neurosci* 2006;26:5591–5603. [PubMed: 16723516]
71. Cafferty WB, Kim JE, Lee JK, et al. Response to correspondence: Kim et al., “Axon regeneration in young adult mice lacking Nogo-A/B.” *Neuron* 38, 187–199. *Neuron* 2007;54:195–199. [PubMed: 17442242]
72. Hasegawa Y, Fujitani M, Hata K, et al. Promotion of axon regeneration by myelin-associated glycoprotein and Nogo through divergent signals downstream of Gi/G. *J Neurosci* 2004;24:6826–6832. [PubMed: 15282288]
73. Bareyre FM, Haudenschield B, Schwab ME. Long-lasting sprouting and gene expression changes induced by the monoclonal antibody IN-1 in the adult spinal cord. *J Neurosci* 2002;22:7097–7110. [PubMed: 12177206]



**Figure 1.** Forelimb Locomotor Scale scores. Both groups showed a significant deficit ( $*P < .05$ ) 1 week postfuniculotomy followed by almost complete recovery by 2 weeks, with no differences between the operated control group ( $n = 7$ ) and the NEP1-40 group ( $n = 6$ ). The catheter delivered either NEP1-40 or vehicle over 4 weeks; cessation of infusion is indicated by the arrow. Data points indicate mean  $\pm$  SEM.

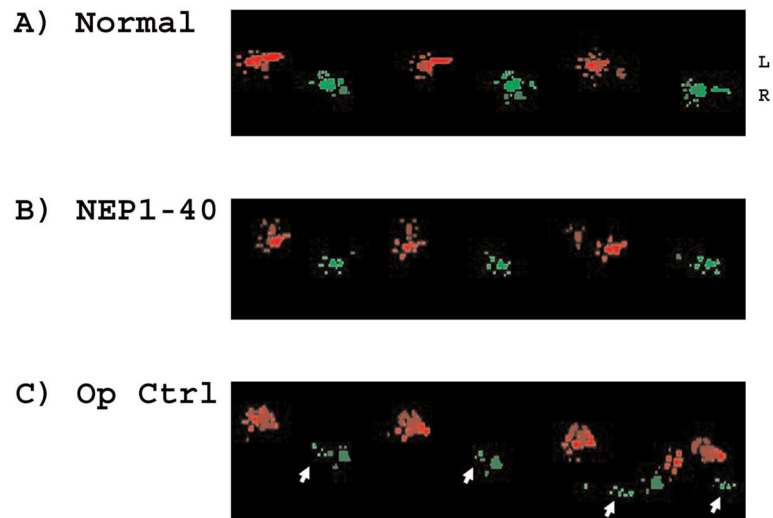




**Figure 2.**

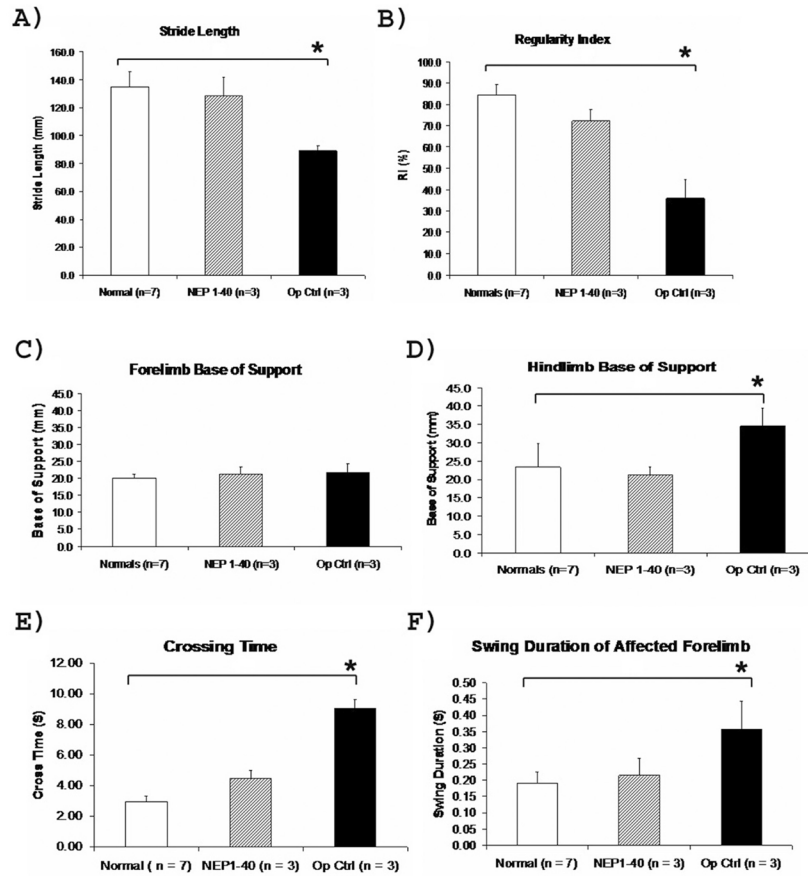
NEP1-40 treatment improved use of the affected forelimb. No deficit was observed 3 days after the catheter implantation, but significant impairment compared to baseline in the use of the affected forelimb was found at 1 week postfuniculotomy in both groups ( $*P < .05$ ). The operated control group ( $n = 7$ ) showed no further recovery. The NEP1-40 group ( $n = 6$ ) demonstrated further significant recovery compared to operation control ( $*P < .05$ ), although performance declined to operation control levels at 8 weeks. Arrow indicates cessation of infusion. Data points indicate mean  $\pm$  SEM.

## Gait Pattern



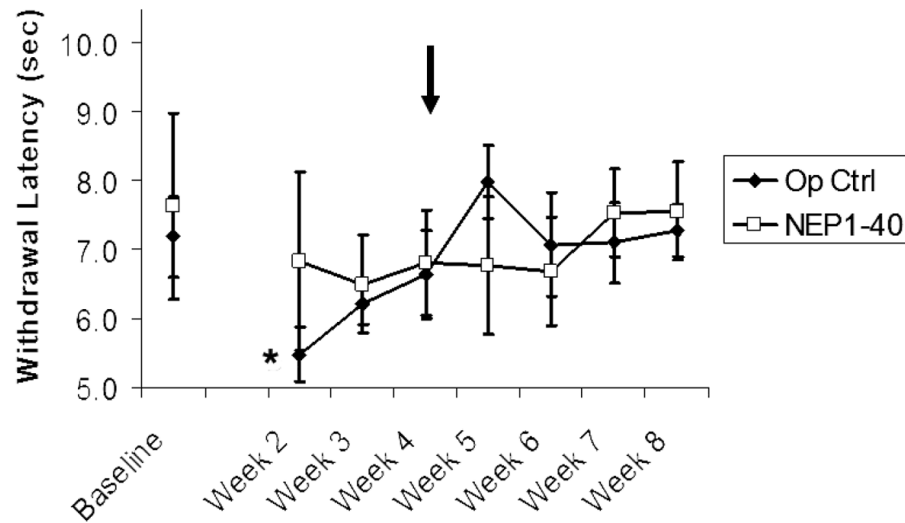
**Figure 3.** NEP1-40-treated animals exhibited stepping parameters similar to normal animals. False color images of steps recorded from the CatWalk at 8 weeks postfuniculotomy in representative (A) normal (n = 7), (B) NEP1-40-treated (n = 3), and (C) operated control (n = 3) animals. (Color coding: bright red = left forepaw; dark red = left hindpaw; bright green = right forepaw; dark green = right hind-paw.) (B) At 8 weeks following NEP1-40 treatment, footprint contact areas were similar in size, and forepaw and hindpaw prints overlapped similar to normals. (C) In the operation control group, right footprints did not overlap (arrows), indicating poor interlimb coordination. Contact area of the right forepaw was decreased in size as the left limbs compensated for the dysfunctional right forelimb.

## Gait Parameters

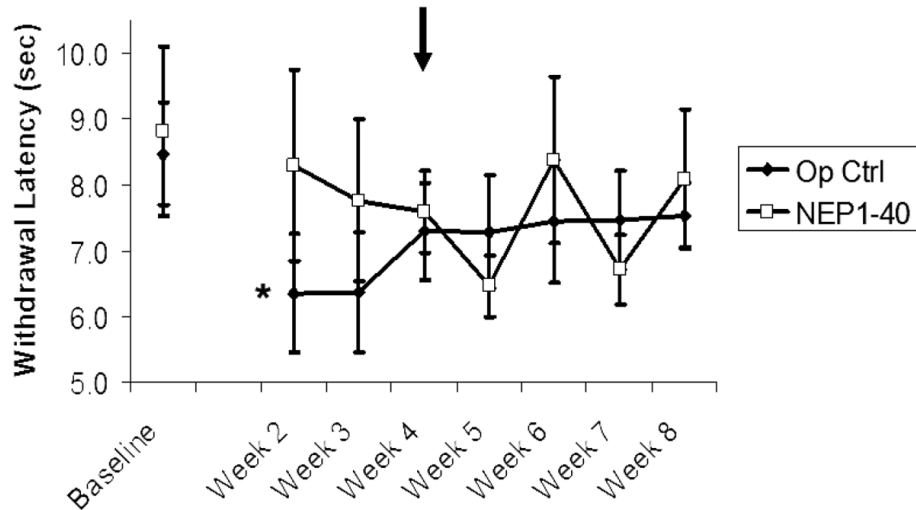
**Figure 4.**

Gait analysis at 8 weeks postfuniclotomy. Data points indicate mean  $\pm$  SEM. NEP1-40 treatment improved gait parameters: (A) Right forelimb stride length in the operated control group decreased compared with normal animals ( $*P < .05$ ); the stride length of the NEP1-40-treated group was similar to normals. (B) Regularity Index decreased in operated controls ( $*P < .05$ ) but was similar to normals after NEP1-40 treatment. (C) Forelimb base of support in both groups of operated animals was similar to normals. (D) Hindlimb base of support increased in operated controls compared to normal animals ( $*P < .05$ ) but not in NEP1-40-treated animals. (E) Crossing time in the operated control group increased compared with normal animals ( $*P < .05$ ). The crossing time of the NEP1-40-treated group was similar to normals. (F) Swing duration of the right forelimb increased in operated controls ( $*P < .05$ ). Swing duration in NEP1-40 rats was similar to normals.

### A) Thermal Sensitivity of the Right Forelimb

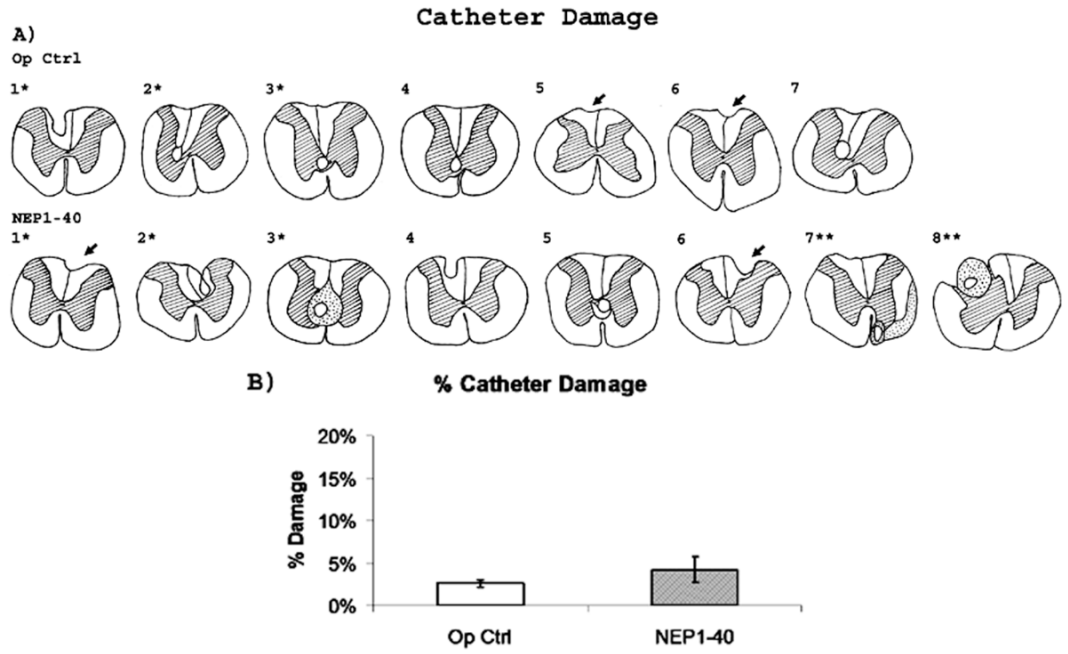


### B) Thermal Sensitivity of the Left Hindlimb



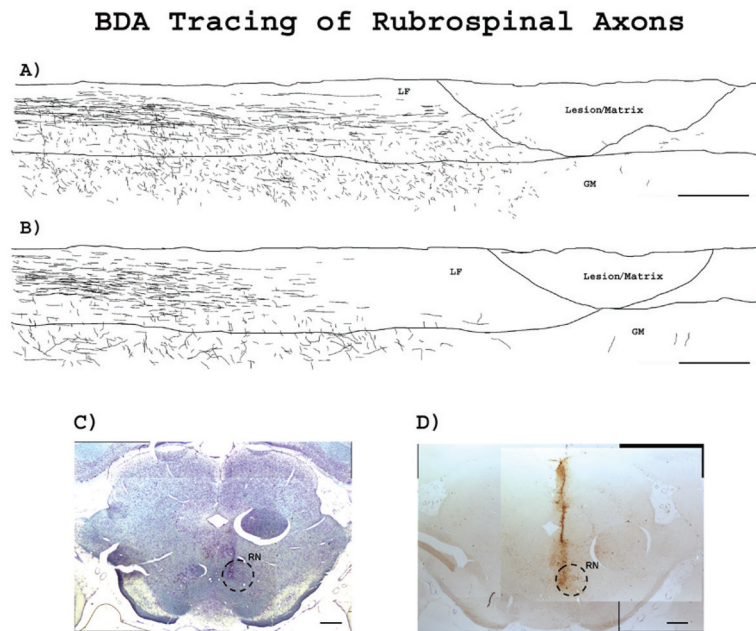
**Figure 5.**

Thermal sensitivity to a heat stimulus. Data points indicate mean  $\pm$  SEM. (A) Thermal sensitivity of the right fore-limb significantly increased in operated controls compared to baseline ( $*P < .05$ ) at 2 weeks postinjury but then recovered to preoperative baseline levels. This increase was not evident in the NEP1-40-treated group. There were no significant differences between groups as they recovered to preoperative baseline levels. (B) Thermal sensitivity of the left hindlimb increased in operated controls ( $*P < .05$ ) at 2 weeks postinjury but then recovered to preoperative baseline levels. This increase was not evident in the NEP1-40-treated group. The catheter delivered either NEP1-40 ( $n = 6$ ) or vehicle ( $n = 7$ ) over 4 weeks as indicated by the arrow.



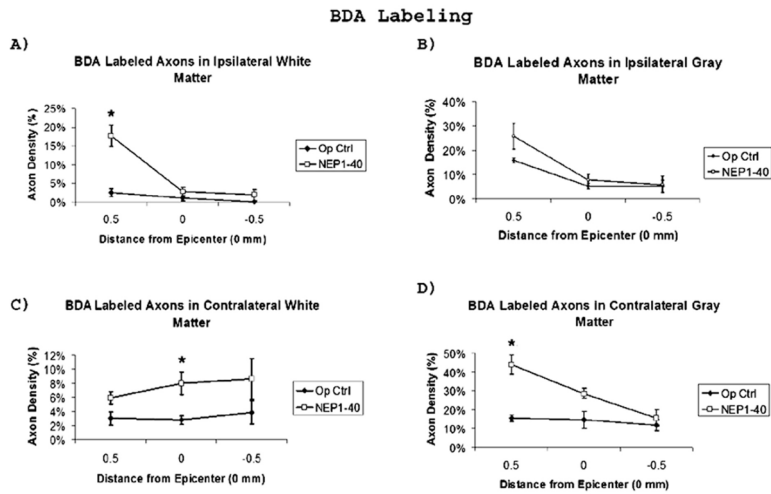
**Figure 6.**

Intrathecal catheterization caused spinal cord damage in both groups. (A) Diagrams show the maximum extent of catheter damage in each animal. The hatched area indicates the gray matter; the stippled area shows dense scar formation. Arrows point to minimal damage to dorsal columns in 2 animals from the operated control (#5, #6) and 2 from the NEP1-40-treated (#1, #6) groups. Two animals in the NEP1-40-treated group (\*\*#7, #8) were removed from the analysis because of the extensive catheter damage to the dorsal and/or ventral column. Three animals from each group (\*#1–3) were chosen at 8 weeks postinjury for the Catwalk analysis (Figures 3 and 4). (B) The area of damage caused by the catheter expressed as the percentage of tissue loss showed no difference in the remaining animals between the operated control (n = 7) and NEP1-40-treated (n = 6) groups.



**Figure 7.**

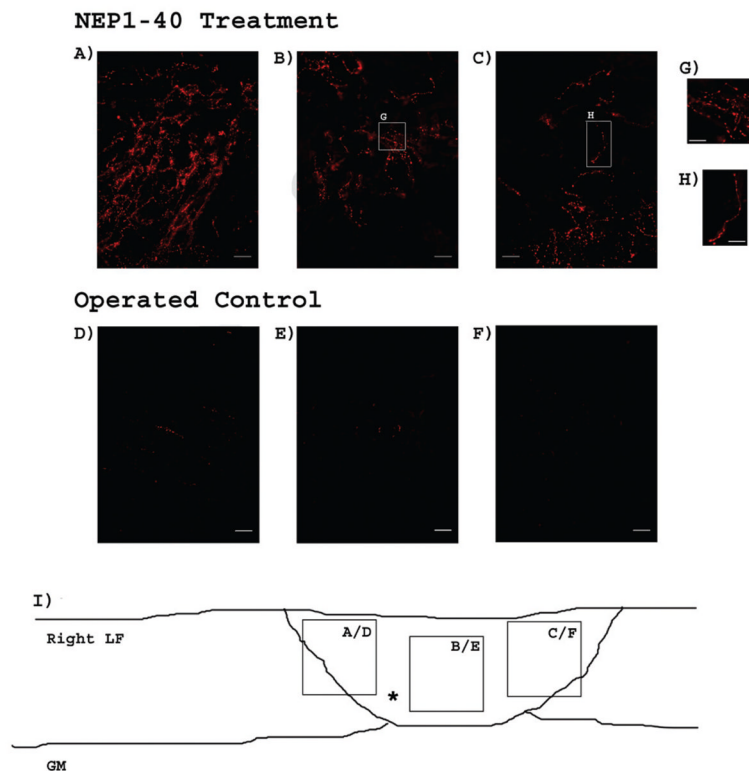
NEP1-40 treatment prevented dieback or promoted growth of BDA-labeled axon. Camera lucida drawings of labeled axons in the ipsilateral lateral funiculus in longitudinal sections from representative (A) NEP1-40 and (B) operated control rats. This composite figure represents stacked drawings made from 21 sections spaced 200  $\mu\text{m}$  apart from each animal. Some axons extended to the rostral edge of the lesion in the NEP1-40 group, but none did in the operated control group. Orientation: right side = rostral to lesion; left side = caudal to lesion. Scale bars = 600  $\mu\text{m}$ . (C) Nissl-myelin staining of the midbrain shows that the needle track reached the red nucleus (circled). Scale bars = 500  $\mu\text{m}$ . (D) BDA staining showed BDA tracer confined to the red nucleus. Scale bars: 500  $\mu\text{m}$ . RN = red nucleus; LF = lateral funiculus; GM = gray matter.



**Figure 8.**

Distribution of BDA-labeled axons around lesion site. To examine the distribution of BDA-labeled axons rostral to, at the epicenter, and caudal to the lesion, axons were counted from (A) ipsilateral lateral funiculus, (B) ipsilateral gray matter, (C) contralateral lateral funiculus, and (D) contralateral gray matter. More BDA-labeled axons were present in the ipsilateral lateral funiculus in the NEP1-40 group rostral to the lesion (A,  $*P < .05$ ). BDA-labeled axons were also increased contralaterally in white (C) and gray (D) matter ( $*P < .05$ ). Data points indicate mean  $\pm$  SEM.

## 5HT Immunocytochemistry

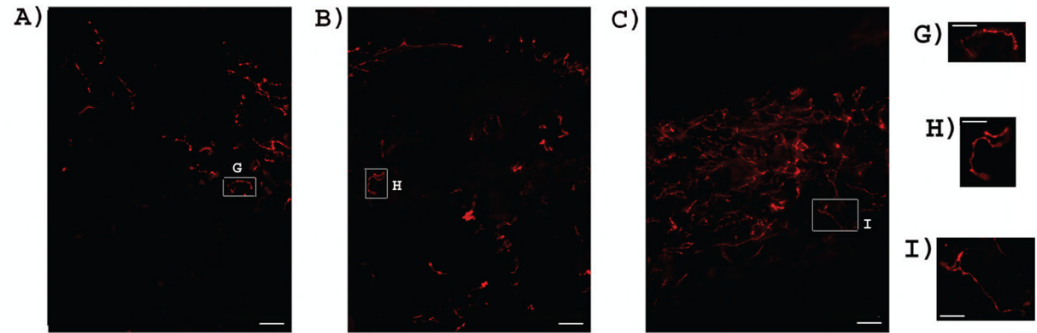
**Figure 9.**

NEP1-40 treatment increased sprouting or regeneration of serotonergic axons into the lesion site. 5-HT positive fibers are present within the lesion site of the NEP1-40-treated group. At 40 $\times$  magnification, more serotonergic axons can be seen in the (A) rostral, (B) middle, and (C) caudal edge of the lesion in the NEP1-40-treated group. Scale bar = 50  $\mu$ m. (G) and (H) indicate a single fiber from image (B) and (C), respectively, shown at twice the magnification. Scale bar = 25  $\mu$ m. The operated control group only showed very few fibers in the (D) rostral edge and (E) middle of the lesion. No serotonergic positive fibers were observed in the (F) caudal edge of the lesion. Scale bar = 50  $\mu$ m. (I) is an illustration that indicates the location of image A/D, B/E, or C/F within the lesion. \*Indicates lesion/matrix site.



## CGRP Immunocytochemistry

### NEP1-40 Treatment



### Operated Control

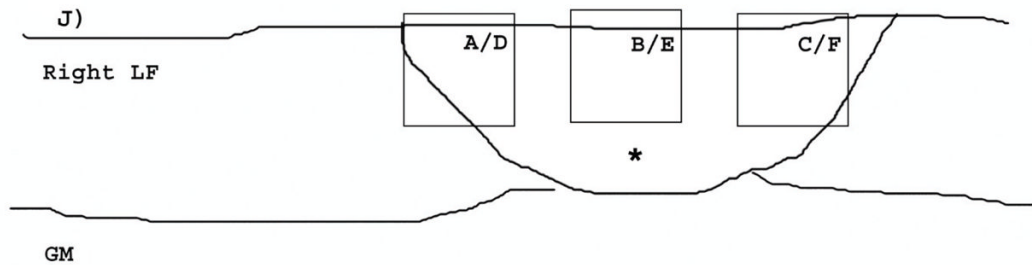
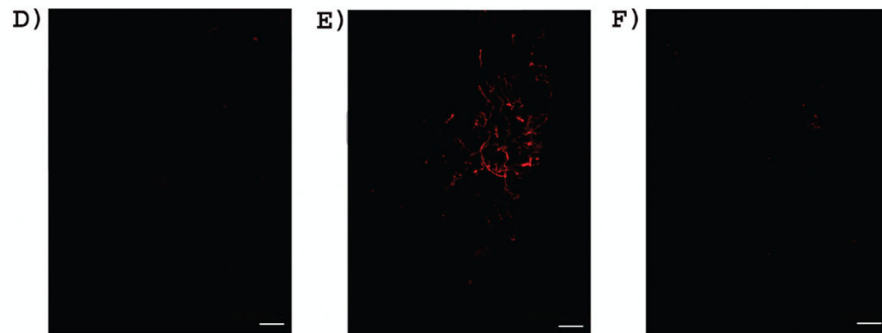


**Figure 10.**

NEP1-40 treatment increased sprouting or regeneration of calcitonin gene-related peptide (CGRP)-positive axons into the lesion site. CGRP-positive fibers are present within the lesion site of the NEP1-40-treated group. At 40 $\times$  magnification, more CGRP axons can be seen in the (A) rostral, (B) middle, and (C) caudal edge of the lesion in the NEP1-40-treated group. Scale bar = 50  $\mu$ m. (G), (H), and (I) indicate a single fiber from image (A), (B), and (C), respectively, shown at twice the magnification. Scale bar = 25  $\mu$ m. The operated control group only showed very few fibers in the (D) rostral, (E) middle, and (F) caudal edge of the lesion. Scale bar = 50  $\mu$ m. (J) is an illustration that indicates the location of image A/D, B/E, or C/F within the lesion. \*Indicates lesion/matrix site.

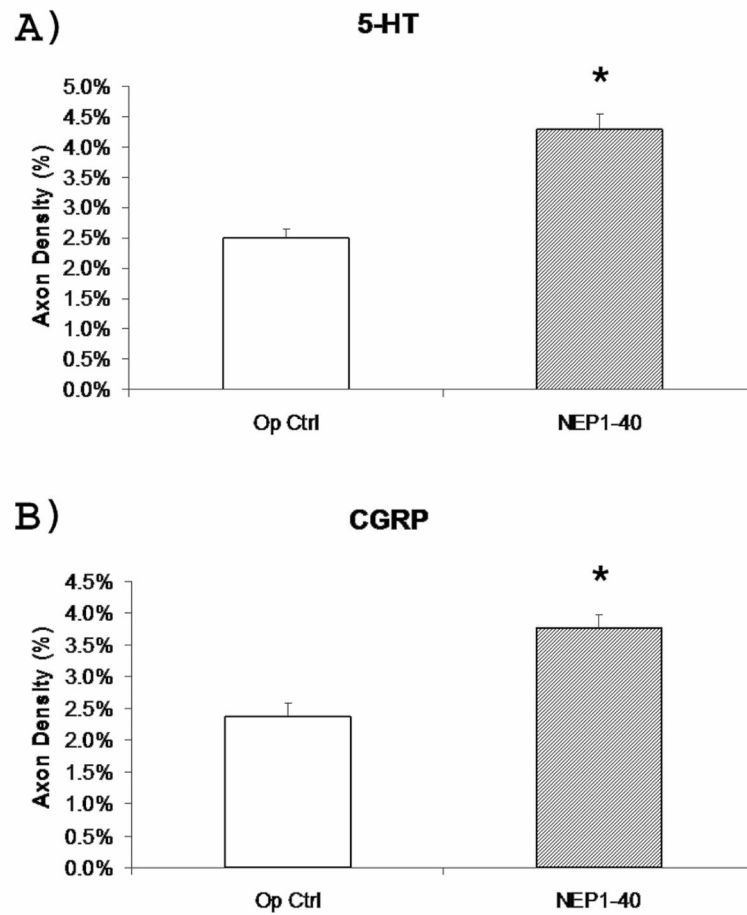


**Figure 11.**

The density of both (A) serotonergic and (B) calcitonin gene-related peptide (CGRP)-positive axons within the lesion/matrix site was increased in the NEP1-40 group ( $*P < .05$ ). Data points indicate mean  $\pm$  SEM.

**Table 1**

## Forelimb Locomotor Scale Score

Score		Score	
0	No movements of the forelimb (shoulder, elbow, or wrist joints)	9	Dorsal stepping and/or occasional plantar stepping
1	Slight movement of 1 or 2 joints of the forelimb	10	Frequent plantar stepping
2	Extensive movement of 1 joint and slight movement of another joint of the forelimb	11	Continuous plantar stepping
3	Slight movement of all 3 joints of the forelimb	12	Continuous plantar stepping with paw position rotated (either at initial contact, liftoff, or both)
4	Extensive movement of 1 joint and slight movement of 2 joints of the forelimb	13	Continuous plantar stepping with paw position parallel (either at initial contact, liftoff, or both)
5	Extensive movement of 2 joints and slight movement of 1 joint of the forelimb	14	Continuous plantar stepping with paw position rotated (either at initial contact, liftoff, or both) and occasional toe clearance
6	Extensive movement of all 3 joints of the forelimb	15	Continuous plantar stepping with paw position parallel (either at initial contact, liftoff, or both) and occasional toe clearance
7	Plantar placement of the forelimb with no weight support	16	Continuous plantar stepping with paw position parallel (either at initial contact, liftoff, or both) with frequent toe clearance
8	Dorsal stepping only	17	Continuous plantar stepping with paw position parallel (either at initial contact, liftoff, or both) and continuous toe clearance

Table 2

## Catheter Damage/Recovery in Cylinder Test

Operated Control	% Damage	Cylinder Test, Average Score of W5-W8	NEP1-40	% Damage	Cylinder Test, Average Score of W5-W8
1	4.9	40.0	1	1.5	61.7
2	1.8	26.0	2	3.0	33.3
3	2.0	19.0	3	11.6	46.1
4	2.0	64.0	4	2.9	75.1
5	1.1	36.5	5	3.1	69.0
6	2.8	60.9	6	3.3	70.1
7	3.5	19.2	7*	10.5	41.5
			8*	11.9	4.6
Mean ± SEM	2.6 ± 0.5	37.5 ± 7.0	Mean ± SEM	4.2 ± 1.5*	59.2 ± 6.6*

\* Data from NEP1-40-treated animals #7 and #8 were excluded from the means presented and all further analysis due to the location of catheter damage.